Journal of Hydrology 578 (2019) 124023

Contents lists available at ScienceDirect

Journal of Hydrology

journal homepage: www.elsevier.com/locate/jhydrol

Research papers

Fine roots determine soil infiltration potential than soil water content in semi-arid grassland soils

Zeng Cui[a,b], Gao-Lin Wu[a,b,c,*], Ze Huang[a], Yu Liu[a,b]

[a] State Key Laboratory of Soil Erosion and Dryland Farming on the Loess Plateau, Northwest A & F University, Yangling, Shaanxi 712100, China
[b] Institute of Soil and Water Conservation, Chinese Academy of Sciences and Ministry of Water Resource, Yangling, Shaanxi 712100, China
[c] CAS Center for Excellence in Quaternary Science and Global Change, Xi'an 710061, China

ARTICLE INFO

This manuscript was handled by G. Syme, Editor-in-Chief

Keywords:
Plant root diameter
Soil infiltration
Soil water content
Infiltration process
Semiarid grassland

ABSTRACT

Soil water is the key limiting factor for achieving sustainable revegetation. Soil infiltration rate plays an important role in determining the inputs from precipitation, which is important for the plant growth and groundwater recharge in semi-arid regions. Soil infiltration rate is generally influenced by belowground biomass (BGB), soil water content (SWC) and other soil properties (total soil porosity, soil mean weight diameter and soil organic carbon). The aim of this study is to understand the effects of plant roots, SWC and other soil properties on soil infiltration rate, and to identify the main factor affecting soil infiltration rate. This study investigated the total soil porosity (TP), soil mean weight diameter (MWD), soil organic carbon (SOC), SWC and plant roots of five grasslands (*Bromus inermis*, *Trifolium repens*, *Panicum virgatum*, *Medicago sativa* and *Miscanthus sinensis*). An automatic measurement system of point source device was used to quantify the soil infiltration rate. Results showed that SWC significantly affected the initial infiltration rate ($P < 0.05$), but plant roots gradually became the main factor affecting soil infiltration rate as the increasing infiltration time. The percentage of root volume (PV) of 0–2 mm was positively correlated with infiltration rate, while the PV of > 4.5 mm was negatively correlated with infiltration rate. Our results indicated that fine roots could increase soil organic matters and form soil pores, thus more determining the potential of soil infiltration than soil water content during the short-term vegetation restoration in semi-arid regions.

1. Introduction

Precipitation infiltration is the main source of soil water replenishment in the semi-arid regions, which influences the vegetation restoration, potential soil erosion and groundwater recharge (Zhao et al., 2013; Leung et al., 2015; Sun et al., 2018). Infiltration is the process of rainfall transform into soil water by downward or gravitational flow (Huang et al., 2017). Soil infiltration capacity could be determined, for example, the initial infiltration rate, steady infiltration rate and mean infiltration rate (Sun et al., 2018). As an important hydrological parameter (Wu et al., 2016), the quantification of infiltration capacity is a crucial issue for vegetation maintenance and land management.

Previous studies have found that soil infiltration capacity was generally affected by various soil properties and vegetation characteristics, such as porosity, organic matters, bulk density and roots (Bormann and Klaassen, 2008; Leung et al., 2015). Franzluebbers (2002) indicated that soil organic matters and soil aggregation improved water infiltration nearly threefold. Alaoui (2015) investigated the hydrological parameters of four representative grassland soils on the Swiss plateau, and found that the interaction between bulk density and macroporsity could facilitate water infiltration. Conversely, some studies have reported that soil bulk density is weakly related to macropore flow (Meek et al., 1989; Fischer et al., 2014). Moreover, soil water content (SWC) is also key factor determining soil infiltration capacity in semi-arid regions (Archer et al., 2002; Zehe and Blöschl, 2004). Cerdà (1996) reported that soil infiltration rate was higher in summer than wet seasons, because of the higher soil moisture contents. Soil water content is susceptible to the changes of external environments, such as rainfall, temperature and vegetation type. In semi-arid regions, the lower initial soil water content increases the potential for infiltration (Alaoui, 2015).

Grassland is the most typical vegetation restoration species in semi-arid areas because of its drought-resistance and good adaptability to severe climate and poor soil conditions (Cui et al., 2018). Grassland had

* Corresponding author at: State Key Laboratory of Soil Erosion and Dryland Farming on the Loess Plateau, Northwest A & F University, NO. 26 Xinong Road, Yangling, Shaanxi Province 712100, China.
E-mail address: wugaolin@nwsuaf.edu.cn (G.-L. Wu).

https://doi.org/10.1016/j.jhydrol.2019.124023
Received 19 April 2019; Received in revised form 4 August 2019; Accepted 6 August 2019
Available online 08 August 2019

abundant root systems which could cause remarkable changes in soil physicochemical properties, and thus had a vital effect on soil infiltration capacity (Fu et al., 2000; Mwendera and Saleem, 2010; Wu et al., 2016). Zhao et al. (2013) evaluated the soil infiltrability of five grasslands of successive age-classes. They found that long-term grassland restoration accumulated organic matter and improved soil structural properties, thus significantly enhancing soil infiltration capacity and reducing soil erosion. The different types of artificial grassland may cause different changes in soil properties and then affect soil infiltration in varying degrees (Angers and Caron, 1998; Bormann and Klaassen, 2008). Huang et al. (2017) found that legume grasslands had higher infiltration capacity than gramineous grasslands in the arid region, which could be attributed to the below-ground biomass (Wu et al., 2016). Legume grasslands had higher below-ground biomass, improving total soil porosity and soil organic matters, thus enhancing soil infiltration capacity. Archer et al. (2002) reported that the abundant root network of grassland could clog the soil pore space and decrease soil infiltration rate. In general, soil infiltration rate was affected by vegetation type, soil porosity, organic matters, soil water content and root system. Previous studies have mainly focused on the effects of soil water content and root biomass on the whole infiltration process. However, the effects of different root diameters on infiltration rate, and the relative importance of root diameter and soil water content during different infiltration stages are poorly understood.

In this study, we measured soil infiltration rate by the point source device at five typical grasslands, i.e., *Bromus inermis*, *Trifolium repens*, *Panicum virgatum*, *Medicago sativa* and *Miscanthus sinensis*. The objectives of this study were to 1) determine the effects of roots diameters and other soil properties (TP, SOC and MWD) on soil infiltration rate; and 2) identify the main factor affecting soil infiltration rate at different infiltration stages. This study could provide the opportunity to clarify the relative importance of root diameter and soil water content during infiltration process, and further provide new insights into soil infiltration for vegetation restoration.

2. Materials and methods

2.1. Experimental site

This study was conducted at the Changwu Agro-ecological Experiment Station of the Chinese Academy of Sciences located at 35°12′–35°16′ N, 107°40′–107°42′ E, and 1215–1226 m altitude, in Changwu County of Shaanxi Province, China. The study area is a typical tableland and gully region on the Loess Plateau, with a mean annual temperature of 9.1 °C. The mean annual precipitation is 584 mm, mostly from July to September, accounting for about 65% of the total annual precipitation. The climate is cold and dry in the winter and spring and hot and rainy in the summer. The mean value of potential annual evaporation is about 1565 mm. The soil in the experiment site (clay: 3.43%, silt: 91.44%, sand: 5.13%) is classified as Heilu soil, belonging to silty sandy loam (Wu et al., 2017b; Cui et al., 2018). The unsaturated soil layer is deep and groundwater is located at a depth of 50–80 m below the soil surface. Since the 1970s, natural vegetation in this area has been gradually substituted by artificial forestlands and grasslands.

2.2. Experimental design

Five typical artificial grasslands were established on the farmland: *Trifolium repens* (*T. repens*), *Bromus* inermis (*B. inermis*), *Panicum virgatum* (*P. virgatum*), *Medicago sativa* (*M. sativa*) and *Miscanthus sinensis* (*M. sinensis*) in 2012. These artificial grasslands were high quality forages which were widely planted in this area. Three replicate plots (3 m × 5 m) were constructed on each grassland type. Various grasses used the same planting time and were irrigated to ensure grass survival during the beginning of the growing period. The amount of flood irrigation in each plot was 3375 kg. Later on, grass growth entirely depended on rainfall, without fertilization or human intervention. This ensured that the conditions in all of the plots were similar but also that any differences were solely due to the grassland type. Therefore, it could be assumed that any differences in soil physical properties and soil water content could be attributed to the type of artificial grassland. All experiment processes were conducted in September 2015, July and September 2016.

2.3. Infiltration measurement

The soil infiltration rates under the different artificial grasslands were determined by a soil infiltration capacity automatic measurement system (Wu et al., 2016; Huang et al., 2017). The automatic measurement system consists of a computer, a camera, a tripod and a peristaltic pump. As the peristaltic pump supplies water to the soil surface at constant rate, the camera automatically captures images of the wet area of soil surface every 3 min under the control of the computer. Soil infiltration rate was calculated by using a numerical algorithm based on the change of wet area.

$$P_n \frac{Q - \sum_{i=1}^{n-1} P_n \Delta S_{n-i+1}}{\Delta Sn} (n = 1, 2, 3) \quad (1)$$

where Q is the rate of water supply, L h^{-1}; P_n is the soil infiltration rate at time n, mm h^{-1}; ΔS_n is the change of the wet area in a given time period ($t_n - t_{n-1}$), mm^2.

The full standing vegetation at ground level was cut off and the litter from the soil surface was removed before measuring. Since soil infiltration rate generally reached a stable level within 75–90 min, we chose 90 min as the time for each infiltration measurement in this study.

According to the dynamic process of infiltration, we took the mean infiltration rate of the first 3 min as the initial infiltration rate (IIR), and then took the average infiltration rate of 3–15 min as the average infiltration rate of stage I (AIRS I). Likewise, the average infiltration rate of stage II (AIRS II) was for the period 15–45 min and the average infiltration rate of stage III (AIRS III) was for the period 45–75 min. The average infiltration rate of the final 15 min (75–90 min) was taken as the steady infiltration rate (SIR).

2.4. Soil sampling and analysis

In each plot, soil samples were collected at soil depth of 10 cm, 20 cm and 30 cm, respectively. These soil samples were taken back to the laboratory to measure soil water content, soil organic carbon, soil bulk and soil aggregates. Among these parameters, soil water content was measured before infiltration measurement, and other parameters were measured after infiltration measurement.

Gravimetric soil water content was measured by using a soil auger (5 cm in diameter) before infiltration measurement. The soil samples were sealed immediately in airtight aluminum cylinders, weighed and brought to the laboratory. Moist soil samples were oven-dried at 105 °C until constant weight for the determination of gravimetric soil water content (unit: g g^{-1}). Volumetric soil water content was calculated using Eq. (3). All the field sampling and laboratory work of soil water content were completed in 3 days.

$$SWC = SWC_g \times BD \quad (2)$$

where SWC is the volumetric soil water content (cm^3 cm^{-3}); BD is the soil bulk density (g cm^{-3}); SWC_g is the gravimetric soil water content (g g^{-1}).

A stainless steel cylindrical ring of 100 cm^3 volume was used for collecting moist soil samples, and oven-dried at105 °C until constant weight for calculating soil bulk density (BD). Total porosity (TP) of soil was calculated using Eq. (1) based on the measured bulk density and

assuming a soil particle density of 2.65 g cm^{-3} (Wu et al., 2016).

$$TP = 1 - \left(\frac{BD}{ds}\right) \times 100 \quad (3)$$

where TP is the total soil porosity (%); BD is the soil bulk density (g cm^{-3}); *ds* is the soil particle density (g cm^{-3}).

The measurement of soil organic carbon (SOC) was determined by oxidation with potassium chromate method (Walkley and Black 1934). Before measuring SOC, soil samples were air-dried at room temperature until constant weight and removed large roots.

The aluminum containers were used to collect undisturbed soil samples after the removal of visible plant residues for the measurement of soil aggregates. Subsequently, all the soil samples were transported to the laboratory within 2 days. Much attention was paid to the soil samples to maintain their structures intact during the transportation. The composition of soil aggregates was determined with the routine dry and wet sieving methods (Liu et al., 1996). The large soil clods, while still moist, were gently broken along natural fracture lines by hand, passed through a 10-mm sieve (Fu et al., 2000), and then air-dried at room temperature for measurement. The air-dried soil samples were sieved manually on a column of five sieves: 5, 2, 1, 0.5 and 0.25 mm, resulting in the collection of six aggregate size fractions: 5–10 mm, 2–5 mm, 1–2 mm, 0.5–1 mm, 0.25–0.5 mm and 0–0.25 mm. The weight percentage of each aggregate-size fraction was calculated. Composite soil samples for wet sieving were made by blending all fractions of dry aggregates proportionally. Exactly 50 g of soil integrated from the above steps was put on the first sieve of the same set in a water bucket containing deionized water and was gently moistened for 30 min so as to drive entrapped air from the aggregates. The aggregates were separated by moving the sieve vertically with a speed of 30 S min^{-1} for 1 min. Lastly, soil fractions remaining on the sieves were separately collected, oven-dried and weighed to get a constant mass. The soil mean weight diameter (MWD) was calculated as follows (Parent et al., 2012).

$$MWD = \sum_{i=1}^{N} \bar{X}_i W_i \quad (4)$$

where X_i is the assumed diameter for *i*th fraction; W_i is the weight fraction remained on the *i*th sieve-size. N is the number of sieves.

2.5. Root parameters measurement

After each infiltration measurement, a flat, square-cornered box (10 cm × 10 cm × 10 cm) was used to sample soil from depth of 0–30 cm and every 10 cm intervals. The soil samples were washed with water for the laboratory measurement of root parameters. Root diameter analyses were measured using WinRHIZO (WinRHIZO Pro 2009b). WinRHIZO is an image analysis system specifically designed for root measurement. It consists of a computer program and image acquisition components, and can be used in morphology (i.e., length, area, and volume), topology, architecture, and color analysis. Then all roots were oven-dried at 75 °C for 48 h until constant weight and weighed for belowground biomass (BGB) after root diameter analysis. The percentage of root volume (PV) of various root diameter sizes was calculated using Eq. (5).

$$PV = \frac{v_i}{V} \quad (5)$$

where *V* is the volume of total roots; V_i is the volume of roots on the *i*th diameter size.

2.6. Statistical analysis

One-way analysis of variance (ANOVA) was employed to analyze the differences of mean values among treatments. Significant differences were determined at the 0.05 level. Unary linear regression and correlation analysis were used to analyze the relationship between roots, SWC, SOC, MWD, TP, and soil infiltration rate. In order to reduce numerous correlated variables down to a smaller number of principal components, principal components analysis (PCA) was used to further investigate the variation in PV. Kaiser–Meyer–Olkin measure (KMO > 0.50) and Bartlett's test of sphericity (P < 0.05) were conducted to test the sampling adequacy of individual and set variables. The selection of main components was determined by the latent root criterion (eigenvalues > 1.0). Kaiser–Meyer–Olkin measure (KMO > 0.50) and Bartlett's test of sphericity were calculated according to Eqs. (6), (7) and (8).

$$KMO = \frac{BB}{AA + BB} \quad (6)$$

$$X^2 = -\left[\frac{n - (2p + 11)}{6}\right] \times \ln[R] \quad (7)$$

$$df = \frac{p(p-1)}{2} \quad (8)$$

where AA is sum of squares of all partial correlation coefficient in partial correlation coefficient matrix; BB is the sum of the squares of the correlation coefficients between all the variables (excluding the variables themselves and themselves); n is the number of data records; p is the number of variables in factor analysis; Ln () is the natural log function; |R| is the value of the correlation coefficient matrix R.

Structural equation model is a statistical method to analyze the relationship between variables based on the covariance matrix of variables, and it is an important tool for multivariate data analysis. We used structural equation model to explain the direct and indirect effect of PC1 and PC2 on soil infiltration through SOC, MWD and TP. Data were fitted to the model using the maximum-likelihood estimation method. The model adequacy was determined by using a Pearson's chi-Square test, Comparative Fit Index (CFI) and Goodness of Fit Index (GFI). Pearson's chi-Square test and Goodness of Fit Index (GFI) belonged to absolute index. Comparative Fit Index (CFI) belonged to relative index. Non-significant Chi-Square test (P > 0.05), high CFI (> 0.9) and GFI (> 0.9) indicate an adequate model fit. All graphs were drawn using the Cor R 3.5.1.

3. Results

3.1. Effects of SWC and other soil properties on infiltration rate

The results of regression analysis showed that the effects of SWC on soil infiltration rate were different at various infiltration stages (Fig. 1). SWC (0–10 cm, 10–20 cm and 20–30 cm) had a significant effect on IIR, AIRS I and AIRS II (P < 0.01). However, SWC of different soil depth had no significant effect on AIRS III and SIR (P > 0.05).

The correlation analysis between the TP, MWD, SOC and infiltration rate were shown in Fig. 2. There was a significant positive correlation between TP and infiltration rate at different infiltration stages (P < 0.01). The correlation analysis revealed that MWD was strongly correlated with AIRS II, AIRS III and SIR (P < 0.05), whereas MWD was not significantly correlated with IIR and AIRS I (P > 0.05). Except for IIR, each infiltration stage (AIRS I, AIRS II, AIRS III and SIR) was significantly correlated with SOC (P < 0.01).

3.2. Effects of roots on infiltration rate

We used regression analysis to investigate the relationship between total root weigh and soil infiltration rate at various infiltration stages (Fig. 3). There was a significant negative correlation between total root weigh and soil infiltration rate (AIRS I, AIRS II, AIRS III and SIR) (P < 0.01), except for IIR. The results of covariance analysis showed that grassland types had a significant effect on soil infiltration rate at different infiltration stages (Table 1).

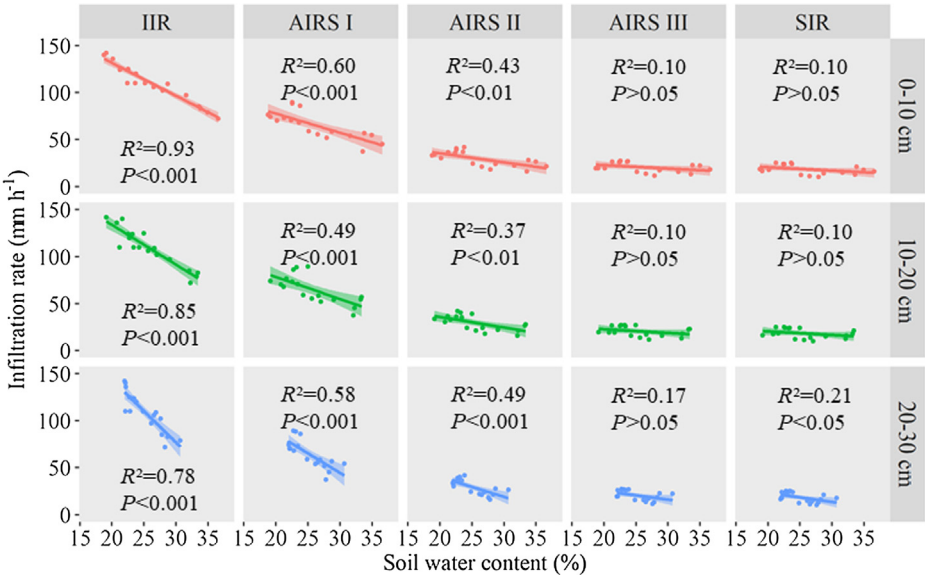

Fig. 1. Regression analysis of soil water content (SWC) and soil infiltration rate at various infiltration stages. AIRS I, AIRS II and AIRS III represent the average infiltration rate of stage I, stage II and stage III, respectively; IIR and SIR represent initial infiltration rate and steady infiltration rate, respectively. The *P* value represents the probability that the original hypothesis is true. The original hypothesis is that the slope of the regression line is zero. $0.01 < P < 0.05$ indicates that there is evidence to reject the original hypothesis. $P < 0.01$ indicates that there is strong evidence to reject the original hypothesis.

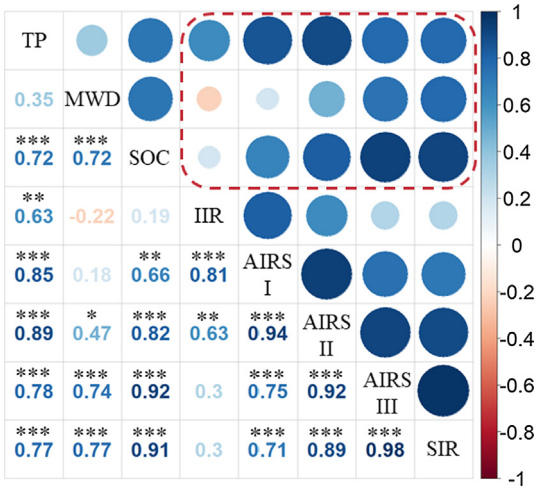

Fig. 2. Correlation analysis of other soil properties (TP, SOC and MWD) and soil infiltration rate at various infiltration stages. Note: TP represents total soil porosity; SOC represents soil organic carbon; MWD represents soil mean weight diameter; AIRS I, AIRS II and AIRS III represent the average infiltration rate of stage I, stage II and stage III, respectively; IIR and SIR represent initial infiltration rate and steady infiltration rate, respectively; * means significant correlation at the 0.05 level ($P < 0.05$); ** means significant correlation at the 0.01 level ($P < 0.01$); *** means significant correlation at the 0.001 level ($P < 0.001$). The *P* value represents the probability that the original hypothesis is true. The original hypothesis is that there is no linear correlation between the two parameters. $0.01 < P < 0.05$ indicates that there is evidence to reject the original hypothesis. $P < 0.01$ indicates that there is strong evidence to reject the original hypothesis.

There were significant differences in the PV of various root diameter sizes among different grasslands ($P < 0.05$; Fig. 4). Both *B. inermis* and *T. repens* showed the highest PV of 0–2 mm root diameter in the soil depth of 0–30 cm (Average: 81.92% and 61.01%, respectively). Whereas *M. sitiva* and *M. sinensis* showed the highest PV of > 4.5 mm root diameter in the soil depth of 0–30 cm (Average: 76.51% and 71.08%, respectively). The PV of various root diameter sizes of *P. virgatum* was relatively well-distributed. Based on this, we conducted a correlation analysis to explain the PV of various root diameter sizes effects of on soil infiltration rate at various infiltration stages (Fig. 5). In the initial infiltration stage, the PV of various root diameter sizes was weakly correlated with infiltration rate ($P > 0.05$). The PV of 0–1 mm and 1–2 mm root diameter was positively correlated with infiltration rate (AIRS II, AIRS III and SIR), and the correlation coefficient increased with infiltration time ($P < 0.01$). In addition, the PV of 2–3 mm and 3–4.5 mm root diameter was weakly correlated with infiltration rate (AIRS I, AIRS II, AIRS III and SIR), while the PV of > 4.5 mm root diameter showed a significant negative correlation with infiltration rate (AIRS II, AIRS III and SIR) and the correlation coefficient increased with infiltration time ($P < 0.01$).

3.3. Relationships between roots, SWC, other soil properties and soil infiltration rate

The parameters with higher weight in the first principal component (PC1) were PV-1, PV-2, and PV-5. The highly loaded parameters in the second principal component (PC2) were PV-3 and PV-4 (Fig. 6). *B. inermis* and *T. repens* had a lower score in PC1, indicating the higher PV (0–2 mm) and lower PV (> 4.5 mm). *P. virgatum* had the lowest score in PC2, indicating the higher PV (2–4.5 mm).

We used a structural equation model to explain the direct and indirect effects of PC1 and PC2 on soil infiltration rate through SOC, MWD and TP. The model taking into account all parameters showed good fit criteria ($\chi^2 = 1.53$, $P = 0.47$; χ^2 $df^{-1} = 0.77$; GFI = 0.96; CFI = 0.97), and 85% of variance in MWD was explained (Fig. 7a). PC1 had a direct negative effect on SOC and MWD, while PC1 had a weak positive effect on TP. PC1had an indirect effect on TP and MWD because of its direct negative effect on SOC. Whereas PC2 had a direct negative effect on MWD, and PC2 showed a weak effect on SOC and TP. Referring to path coefficient, PC1 had the strongest direct or indirect effect on SOC, TP and MWD, far greater than PC2.

The relationship of SWC, MWD, TP and soil infiltration rate were shown in Fig. 7. The final model explained > 83% of variance in soil infiltration rate with good fit criteria ($\chi^2 = 0.84$, $P = 0.36$; χ^2 $df^{-1} = 0.338$; GFI = 0.97; CFI = 0.98). In the initial infiltration stage, SWC showed a significantly negative correlation with infiltration rate, while the TP was weakly correlated with IIR. As the infiltration time increased, the impacts of SWC on infiltration rate gradually decreased, whereas the TP and MWD significantly affected infiltration rate. Referring to path coefficient of −0.81, SWC had the strongest direct effect on IIR, much more than other parameters. The results revealed that the direct effect of TP upon AIRS I and AIRS II (r = 0.74; r = 0.76) was nearly three times that of MWD and SWC (Fig. 6c and d). MWD and TP showed the similar importance on affecting SIR.

PC1 and PC2 had an indirect effect on soil infiltration rate at

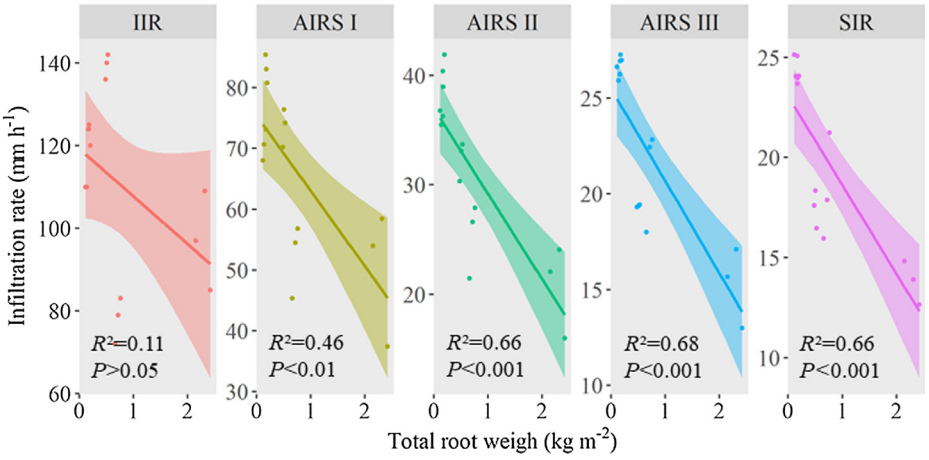

Fig. 3. Regression analysis of total root weigh and soil infiltration rate at various infiltration stages. AIRS I, AIRS II and AIRS III represent the average infiltration rate of stage I, stage II and stage III, respectively; IIR and SIR represent initial infiltration rate and steady infiltration rate, respectively. The *P* value represents the probability that the original hypothesis is true. The original hypothesis is that the slope of the regression line is zero. $0.01 < P < 0.05$ indicates that there is evidence to reject the original hypothesis. $P < 0.01$ indicates that there is strong evidence to reject the original hypothesis.

Table 1
Results of covariance analysis of variables that significantly affecting soil infiltration rate.

		df	F	p
Dependent variable	IIR			
Covariate	BGB	1 7	0.01	0.91
Fixed factor	Grassland types	4 7	24.49	< 0.001
Dependent variable	AIRS I			
Covariate	BGB	1 7	0.51	0.50
Fixed factor	Grassland types	4 7	6.40	0.02
Dependent variable	AIRS II			
Covariate	BGB	1 7	1.00	0.35
Fixed factor	Grassland types	4 7	5.92	0.02
Dependent variable	AIRS III			
Covariate	BGB	1 7	0.35	0.57
Fixed factor	Grassland types	4 7	6.43	0.02
Dependent Variable	SIR			
Covariate	BGB	1 7	0.22	0.65
Fixed factor	Grassland types	4 7	6.56	0.02

Note: IIR represents initial infiltration rate; AIRS I, II and III represent the average infiltration rate in stage I, II and III, respectively; SIR represents steady infiltration rate. BGB represents the below-ground biomass.

different infiltration stages through its direct or indirect effect on SOC, TP and MWD. Therefore, soil infiltration rate was influenced by PC1, PC2 and SWC. As the increase of infiltration time, the impacts of SWC on infiltration rate gradually weakened, while the impacts of PC1 and PC2 on infiltration rate gradually increased. SWC was the main factor affecting the steady infiltration rate. Referring to path coefficient, PC1 was the main factor affecting the steady infiltration rate, far exceeding than those of SWC and PC2 on steady infiltration rate.

4. Discussion

It is well known that soil infiltration capacity is generally controlled by both vegetation characteristics and soil physical properties (Leung et al., 2015). Many studies have reported that below-ground biomass, soil water content, soil organic matters, total soil porosity and soil aggregate are the main factors to determine the soil infiltration capacity (Huang et al., 2017; Wu et al., 2016). In the present study, we conducted a regression and correlation analysis to determine the relationship between roots, SOC, MWD, TP, and soil infiltration rate at various infiltration stages. The results showed that there was a significantly positive correlation between other soil properties (SOC, MWD and TP) and soil infiltration rate (AIRS II, AIRS III and SIR). This was consistent with Wu et al., (2016) who found that the higher soil porosity increased the soil infiltration capacity in semiarid region. Huang et al. (2017) also found that TP, SOC and soil aggregate were the vital factor for stable change stage of infiltration rates, and the increased soil porosity, SOC and soil aggregate would improve infiltration capacity (Neris et al., 2012; Zhao et al., 2013; Fischer et al., 2014). Roots system plays a most important role in soil infiltration process, and higher infiltration rate is related to higher BGB (Huang et al., 2017). However, this was not consistent with our results that total root weight had a significantly negative effect on soil infiltration rate (Fig. 3). Therefore, a covariance analysis was conducted to explain this problem follows.

The results showed that both grassland types had a significant effect on soil infiltration rate at various infiltration stages ($P < 0.05$, Table 1). Based on this, we conducted a correlation analysis to compare the differences in root distribution characteristics of different grassland types (Fig. 4). These could be attributed that *T. repens* and *B. inermis* had higher volume ratio of 0–2 mm root diameter (Average: 81.92% and 61.01%, respectively), while *M. sitiva* and *M. sinensis* had more coarse roots (Fig. 2). Root characteristics (i.e., root diameter and root distribution) could explain the differences of infiltration capacity among different species (Huang et al., 2017; Leung et al., 2017; Wu et al., 2017a). The results showed that there was a significantly positive correlation between the PV of 0–2 mm root diameter and soil infiltration rate (AIRS II, AIRS III and SIR). In addition, the PV of 2–4.5 mm root diameter was weakly correlated with infiltration rate, while the PV of > 4.5 mm root diameter showed a significantly negative correlation with infiltration rate (AIRS II, AIRS III and SIR). The decomposition of roots could increase soil infiltration capacity (Fischer et al., 2014; Luna et al., 2017). Root diameter is a key factor determining root decomposition, because it integrates both chemical and physical properties associated with root development. Coarse roots differ markedly from fine roots in decomposition rate. Zhang and Wang (2015) found that fine roots decomposed significantly faster than coarse roots in middle latitude areas, which could prove that our results were reasonable. Fine roots track changes in aboveground phenology, and temperature, moisture and nutrient in soils (Cheng and Bledsoe, 2002), with consequent seasonal changes in biomass and distribution and high annual turnover rates (Wells and Eissenstat, 2001; Eissenstat et al., 2000). Coarse roots decayed depending on climate, especially annual temperature and annual rainfall, than did fine root (Zhang and Wang 2015).

Many studies have reported that plant rooting features are closely related to the changes in soil structure and in turn influence soil infiltration capacity during vegetation restoration (Neris et al., 2012;

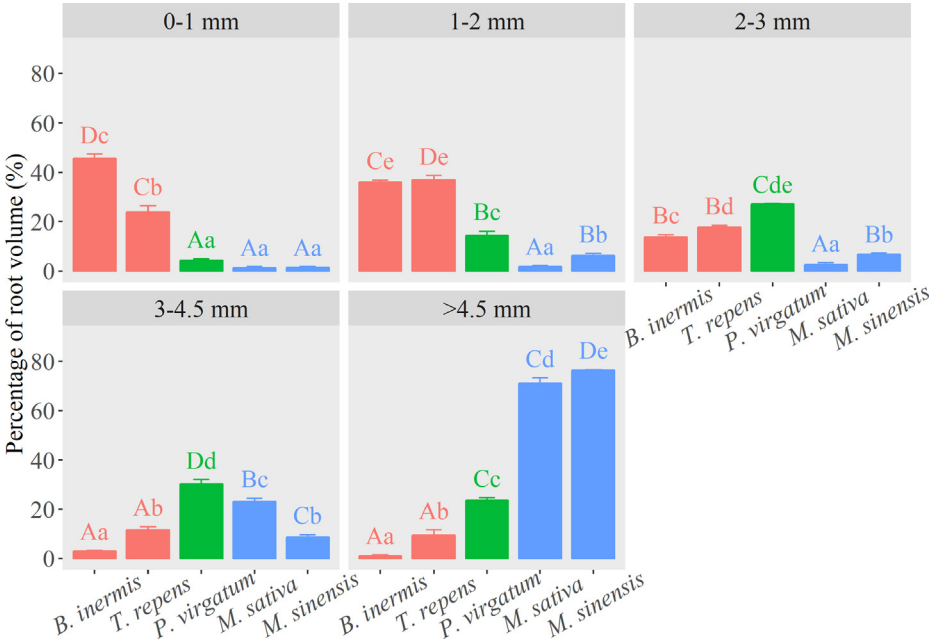

Fig. 4. Percentage of root volume (PV) of different root diameter sizes in different artificial grasslands. Note: The different lowercase letters mean the significant differences at different artificial grasslands, the different capital letters mean the significant differences at distribution of different root diameter ($P < 0.05$). The P value represents the probability that the original hypothesis is true. The original hypothesis is that there is no difference among the data. $0.01 < P < 0.05$ indicates that there is evidence to reject the original hypothesis. $P < 0.01$ indicates that there is strong evidence to reject the original hypothesis.

Fig. 5. Correlation analysis of percentage of root volume (PV) and soil infiltration rate at various infiltration stages. Note: PV-1 represents PV of 0–1 mm; PV-2 represents PV of 1–2 mm; PV-3 represents PV of 2–3 mm; PV-4 represents PV of 3–4.5 mm; PV-5 represents PV of > 4.5 mm; AIRS I, AIRS II and AIRS III represent the average infiltration rate of stage I, stage II and stage III, respectively; IIR and SIR represent initial infiltration rate and steady infiltration rate, respectively; * means significant correlation at the 0.05 level ($P < 0.05$); ** means significant correlation at the 0.01 level ($P < 0.01$); *** means significant correlation at the 0.001 level ($P < 0.001$). The P value represents the probability that the original hypothesis is true. The original hypothesis is that there is no linear correlation between the two parameters. $0.01 < P < 0.05$ indicates that there is evidence to reject the original hypothesis. $P < 0.01$ indicates that there is strong evidence to reject the original hypothesis.

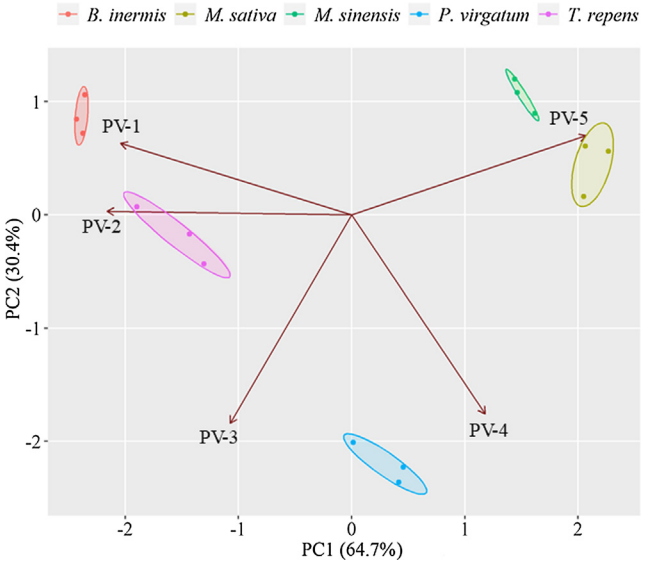

Fig. 6. The load of the principal component calculated by principal component analysis. Two PCA components explain 95.1% of the variance in Soil physical properties. Note: PV-1 represents PV of 0–1 mm; PV-2 represents PV of 1–2 mm; PV-3 represents PV of 2–3 mm; PV-4 represents PV of 3–4.5 mm; PV-5 represents PV of > 4.5 mm.

Huang et al., 2017; Wu et al., 2016). Roots enmesh and realign soil particles and release exudates, which result in the modifications of soil properties and enhancing aggregation (Bronick and Lal, 2005). Fischer et al., (2014) indicated that decaying roots increased soil organic matters and formed soil pores, and thus influenced infiltration capacity due to change in burrowing activity and biomass of earthworms. In the present study, soil water content had the strongest direct effect on IIR (Fig. 7b). This was consistent with Alaoui (2015) who found that the lower initial soil water content increased the potential for soil infiltration rate in semiarid regions. The topsoil was dry, which would accelerate infiltration rate at the initial stage. As the increase of infiltration time, soil water content gradually increased, thus the infiltration rate was greatly affected by other factors. The results showed that AIRS III and SIR were directly affected by both TP and MWD (Fig. 7e and f), and the direct positive effect of TP upon AIRS III (r = 0.72) was more than twice that of MWD (r = 0.33). Soil pores are the channels of preferential flow, promoting vertical water movement towards deeper horizons (Luna et al., 2017). Van Schaik (2009) reported that root channels improved the soil porosity, resulting in higher infiltration capacity than expected. The results showed that the PC1 had an indirect effect on soil infiltration rate (AIRS II, AIRS III and SIR) because of its direct or indirect effect on SOC, TP and MWD, which was much more than PC2 (Fig. 7). Decomposition of mature roots increased soil organic matters and formed soil pores, which promoted vertical water movement towards deeper horizons and thus influenced

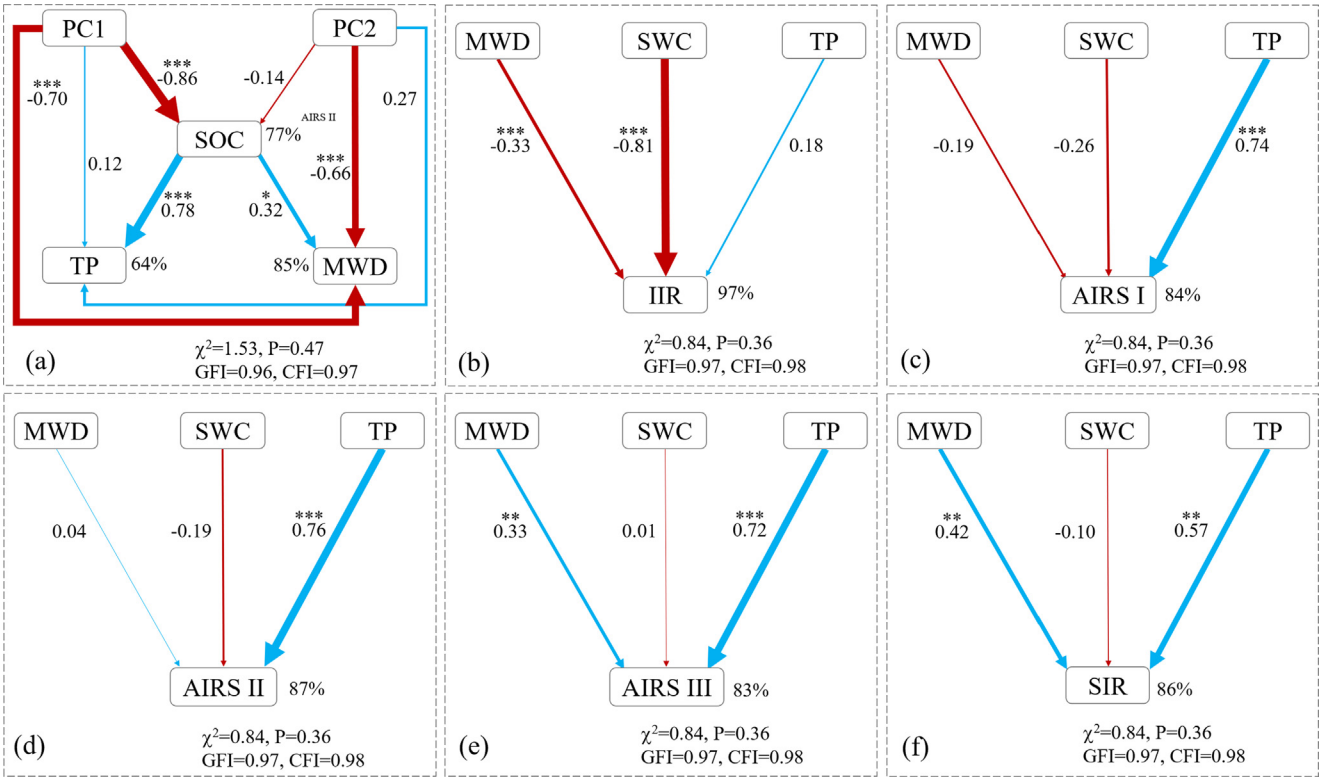

Fig. 7. Structural equation models demonstrating the effects of plant roots on other soil properties (a), the effects of other soil properties (TP, SOC and MWD) and soil water content on soil infiltration rate at various infiltration stages (b–f). The rectangles and single-headed arrows represent indicators and causal effects, respectively. The numbers near arrows indicate the standardized path coefficients. Minus values indicated negative effects. Positive values indicate positive effects. Note: PC1 and PC2 represent the score of principal component 1 and principal component 2; TP represents total soil porosity, SOC represents soil organic carbon; MWD represents soil mean weight diameter; SWC represents the soil water content; AIRS I, AIRS II and AIRS III represent the average infiltration rate of stage I, stage II and stage III, respectively; IIR and SIR represent initial infiltration rate and steady infiltration rate, respectively.

infiltration capacity (Fischer et al., 2014; Luna et al., 2017). Many studies have reported that root decomposition represents a large carbon cost to plants, and serves as a potential soil organic matter source (John et al., 2002; Zhang and Wang, 2015; Redelstein et al., 2018). Fine roots have the high decomposition rate, increasing soil porosity and soil organic matters, thus enhanced soil infiltration capacity. In semiarid areas where dry and rainless, non-perishable coarse roots can compact soil and block water flow, thereby decreasing soil infiltration rate. This negative effect masked the positive effect of fine root to a certain extent, leading to the result that total root weigh was negative correlated with soil infiltration rate differing from previous studies (Fig. 3).

In conclusion, our results show that soil infiltration rate was affected by both soil water content and PV. SWC was the main factor affecting the initial infiltration rate, far exceeding those of PV on initial infiltration rate. As the increase of infiltration time, the impacts of SWC on infiltration rate gradually weakened, while the impacts of PV on infiltration rate gradually increased. PV of 0–2 mm and > 4.5 mm was the main factor affecting the steady infiltration rate, far exceeding than those of SWC and PV of 2–4.5 mm on steady infiltration rate. Although our results determined the effects of PV and soil water content on soil infiltration during the whole process, there are still some limitations. The results of the relationship between PV and infiltration capacity, which are based on short-term experiment in semiarid regions, should be treated with great caution: the factors that best correlate with rates of early root decomposition are often not the same as those related to long-term root decomposition. Consequently, further research is needed to clarify the relationship between root diameter and infiltration response during long-term vegetation restoration in semiarid regions.

5. Conclusion

In conclusion, our results show that soil infiltration rate is affected by both SWC and PV during infiltration process. Fine roots (0–2 mm of root diameter) were positively correlated with infiltration rate, while coarse roots (> 4.5 mm of root diameter) were negatively correlated with infiltration rate. Soil water content is negatively related to soil infiltration rate, but the impacts of soil water content on soil infiltration gradually weaken as the increase of infiltration time. PV is the main factor influencing infiltration rate with the increasing infiltration time. The results contribute to clarify the relative importance of PV and soil water content during infiltration process and provide new insights into soil infiltration for vegetation restoration in semiarid region.

Declaration of Competing Interest

The authors declare that they have no known competing financial interests or personal relationships that could have appeared to influence the work reported in this paper.

Acknowledgements

We thank the editors and anonymous reviewers for their constructive comments and suggestions on this manuscript, and also thank He Honghua for improving the language of this article. This research was funded by the Projects of National Natural Science Foundation of China (NSFC 41722107), the Light of West China Program of Chinese Academy of Sciences (XAB2015A04, XAB2018B09), and the Youth Talent Plan Foundation of Northwest A&F University (2452018025).

References

Alaoui, A., 2015. Modelling susceptibility of grassland soil to macropore flow. J. Hydrol. 525, 536–546.

Angers, D.A., Caron, J., 1998. Plant-induced changes in soil structure: processes and feedbacks. Biogeochemistry 42, 55–72.

Archer, N.A.L., Quinton, J.N., Hess, T.M., 2002. Below-ground relationships of soil texture, roots and hydraulic conductivity in two-phase mosaic vegetation in South-east Spain. J. Arid Environ. 52, 535–553.

Bormann, H., Klaassen, K., 2008. Seasonal and land use dependent variability of soil hydraulic and soil hydrological properties of two Northern German soils. Geoderma 145, 295–302.

Bronick, C.J., Lal, R., 2005. Soil structure and management: a review. Geoderma 124, 3–22.

Cerdà, A., 1996. Seasonal variability of infiltration rates under contrasting slope conditions in southeast Spain. Geoderma 69, 217–232.

Cheng, X.M., Bledsoe, C.S., 2002. Contrasting seasonal patterns of fine root production for blue oaks (*Quercus douglasii*) and annual grasses in California oak woodland. Plant Soil 240, 263–274.

Cui, Z., Liu, Y., Jia, C., Huang, Z., He, H.H., Han, F.P., Shen, W.B., Wu, G.L., 2018. Soil water storage compensation potential of herbaceous energy crops in semi-arid region. Field Crop Res. 223, 41–47.

Eissenstat, D.M., Wells, C.E., Yanai, R.D., Whitbeck, J.L., 2000. Building roots in a changing environment, implications for root longevity. New Phytol. 147, 33–42.

Franzluebbers, A.J., 2002. Water infiltration and soil structure related to organic matter and its stratification with depth. Soil Till. Res. 66, 197–205.

Fischer, C., Roscher, C., Jensen, B., Eisenhauer, N., Baade, J., Attinger, S., Scheu, S., Weisser, W.W., Schumacher, J., Hildebrandt, A., 2014. How do earthworms, soil texture and plant composition affect infiltration along an experimental plant diversity gradient in grassland? PLoS One 9, e98987.

Fu, B.J., Chen, L.D., Ma, K.M., Zhou, H.F., Wang, J., 2000. The relationships between land use and soil conditions in the hilly area of the loess plateau in northern Shaanxi, China. Catena 39, 69–78.

Huang, Z., Tian, F.P., Wu, G.L., Liu, Y., Dang, Z.Q., 2017. Legume grasslands are in favour of promoting precipitation infiltration than gramineous grasslands in the arid regions: legume grasslands promoting precipitation infiltration. Land Degrad. Dev. 28, 309–316.

John, B., Pandey, H.N., Tripathi, R.S., 2002. Decomposition of fine roots of pinus kesiya and turnover of organic matter, n and p of coarse and fine pine roots and herbaceous roots and rhizomes in subtropical pine forest stands of different ages. Biol. Fert. Soil 35, 238–246.

Leung, A.K., Boldrin, D., Liang, T., Wu, Z.Y., Kamchoom, V., Bengough, A.G., 2017. Plant age effects on soil infiltration rate during early plant establishment. Géotechnique 68, 646–652.

Leung, A.K., Garg, A., Coo, J.L., Ng, C.W.W., Hau, B.C.H., 2015. Effects of the roots of Cynodon dactylon and Schefflera heptaphylla on water infiltration rate and soil hydraulic conductivity. Hydrol. Process. 29, 3342–3354.

Liu, G.G., Jiang, N.H., Zhang, L.D., Liu, Z.L., 1996. Soil Physical and Chemical Analysis and Description of Soil Profiles. Standard Press of China, Beijing.

Luna, L., Vignozzi, N., Miralles, I., Solé-Benet, A., 2017. Organic amendments and mulches modify soil porosity and infiltration in semiarid mine soils. Land Degrad. Dev. 29, 1019–1030.

Meek, B.D., Rechel, E.A., Carter, L.M., DeTar, W.R., 1989. Changes in infiltration under alfalfa as influenced by time and wheel traffic. Soil Sci. Soc. Am. J. 53, 238–241.

Mwendera, E.J., Saleem, M.A.M., 2010. Infiltration rates, surface runoff, and soil loss as influenced by grazing pressure in the Ethiopian highlands. Soil Use Manag. 13, 29–35.

Neris, J., Jiménez, C., Fuentes, J., Morillas, G., Tejedor, M., 2012. Vegetation and landuse effects on soil properties and water infiltration of Andisols in Tenerife (Canary Islands, Spain). Catena 98, 55–62.

Parent, L.E., Almeida, C.X.E., Hernandes, A., Egozcue, J.J., Gülser, C., Bolinder, M.A., Kätterer, T., Andrén, O., Parent, S.E., Anctil, F., Centurion, J.F., Natale, W., 2012. Compositional analysis for an unbiased measure of soil aggregation. Geoderma 179, 123–131.

Redelstein, R., Dinter, T., Hertel, D., Leuschner, C., 2018. Effects of inundation, nutrient availability and plant species diversity on fine root mass and morphology across a saltmarsh flooding gradient. Front Plant Sci. 9, 98.

Sun, D., Yang, H., Guan, D.X., Yang, M., Wu, J.B., Yuan, F.H., Jin, C.J., Wang, A.Z., Zhang, Y.S., 2018. The effects of land use change on soil infiltration capacity in China: a meta-analysis. Sci. Total Environ. 626, 1394–1401.

van Schaik, N.L.M.B., 2009. Spatial variability of infiltration patterns related to site characteristics in a semi-arid watershed. Catena 78, 36–47.

Wells, C.E., Eissenstat, D.M., 2001. Marked differences in survivorship among apple roots of different diameters. Ecology 82, 882–892.

Wu, G.L., Yang, Z., Cui, Z., Liu, Y., Fang, N.F., Shi, Z.H., 2016. Mixed artificial grasslands with more roots improved mine soil infiltration capacity. J. Hydrol. 535, 54–60.

Wu, G.L., Liu, Y., Yang, Z., Cui, Z., Deng, L., Chang, X.F., Shi, Z.H., 2017a. Root channels to indicate the increase in soil matrix water infiltration capacity of arid reclaimed mine soils. J. Hydrol. 546, 133–139.

Wu, J.H., Zhu, D.D., Wang, H.Y., Yang, T., Liu, Y.W., 2017b. Effect of different types humic acid class on erosion and nutrient loss on loess slope. J. Soil Water Conserv. 31, 24–29.

Zehe, E., Blöschl, G., 2004. Predictability of hydrologic response at the plot and catchment scales: role of initial conditions. Water Resour. Res. 40, 497–518.

Zhang, X.Y., Wang, W., 2015. The decomposition of fine and coarse roots: their global patterns and controlling factors. Sci. Rep. 5, 9940.

Zhao, Y.G., Wu, P.T., Zhao, S.W., Feng, H., 2013. Variation of soil infiltrability across a 79-year chronosequence of naturally restored grassland on the loess plateau. China. J. Hydrol. 504, 94–103.